IEEE Access
Multidisciplinary | Rapid Review | Open Access Journal

Received June 23, 2020, accepted July 9, 2020, date of publication July 13, 2020, date of current version July 23, 2020.

Digital Object Identifier 10.1109/ACCESS.2020.3008911

Optimization of Water Distribution Network Design for Resisting Cascading Failures

QING SHUANG[1], CHAO RAN HUANG[1], AND JUN WANG[2]
[1]Department of Construction Management, School of Economics and Management, Beijing Jiaotong University, Beijing 100044, China
[2]Department of Civil and Environmental Engineering, Mississippi State University, Starkville, MS 39762, USA

Corresponding author: Qing Shuang (qings@bjtu.edu.cn)

This work was supported in part by the National Natural Science Foundation of China under Grant 71501008, in part by the Beijing Social Sciences Foundation under Grant 18GLC070, in part by the Ministry of education of Humanities and Social Science Foundation under Grant 20YJC630121, in part by the Fundamental Research Funds for the Central Universities under Grant 2019JBW007, and in part by the China Scholarship Council under Grant 201707095080.

ABSTRACT Water distribution networks (WDNs) is crucial to ensure social operations and economic activities. However, WDNs are highly sensitive and vulnerable to disasters. The aim of this study is to mitigate the catastrophic consequences of cascading failures in WDNs. A flow-based WDN cascading failure model is built. The extended multi-objective particle swarm optimization model is developed to resist cascading failures and improve resilience. This model takes pipe diameter as the decision variable to minimize cost and maximize pressure deficit. Water balance, pressure, and standard pipe diameter are the constraints. The classical optimal scenario (COS) and the cascading failure scenario (CFS) are simulated. The model is applied to a small and medium-sized benchmarked WDN. Results show that the extended PSO can find the optimal solution on the benchmarked WDN. The Pareto fronts are obtained. Compare to the Pareto fronts between COS and CFS, the pressure deficit under CFS is significantly reduced, and the cost is reduced while the same pressure deficit increased. Different tolerance parameters are tested. The small network is not sensitive to the tolerance parameter, but the medium-sized network is sensitive. The model evaluates a variety of conflicting goals, which help designers and water managers resist cascading failures in WDNs.

INDEX TERMS Water distribution networks, cascading failure, pressure deficit, multi-objective optimization model, particle swarm algorithm.

I. INTRODUCTION

A water distribution network (WDN) is a critical part of a water supply system, which is a critical infrastructure system. A WDN consists of several components such as pipes, reservoirs, and hydraulic devices. Each component is selected based on a trade-off between technical and economic considerations [1]. The network as a whole is required to supply and satisfy the demands and pressure at given points with cost-effective design.

Since the mid-1970s, advances had been made in WDN simulation and optimization [2]. They provided promising and useful decision support tools for WDN design and performance evaluation. The initial WDN design optimization was a single-objective problem; that is, WDNs focused on the minimum cost with conditions on meeting the minimum pressure or economic flow velocities [3]. However, this problem did not consider other objectives such as nodal pressure, water quality, or vulnerability [3]. The best solution for cost may result in low performance under uncertainties such as pipe bursts, power outages, or pipe aging.

Because of these shortcomings of the single-objective problem, the multi-objective design of WDNs has received increasing attention to identify the trade-off between cost and performance. Multi-objective design is a nonlinear, discrete, and large-scale optimization problem. Heuristic algorithms have been proven effective in searching and finding effective solutions for such problems [4]. Multi-objective heuristic algorithms have been widely applied in WDN design problems because of their promising performance compared to traditional optimization algorithms. They are easy to understand and implement and can handle nonlinear and

The associate editor coordinating the review of this manuscript and approving it for publication was Dusmanta Kumar Mohanta.

discrete problems. Further, these population-based methods can obtain several non-dominated solutions in a run. The searched Pareto-optimal front is more complex and difficult to implement for other methods such as linear programming and gradient search [5].

Mehdi and Asghar [6] adjusted the node pressure with the particle swarm optimization algorithm considering both the pressure reducing valves and the reliability of WDNs. Zhang *et al.* [7] optimized the locations of water meters based on natural and administrative borders using the genetic algorithm to improve the hydraulic ability and water quality of WDNs. Zheng *et al.* [8] developed a parameter-adaptive strategy based on an ant colony optimization algorithm to solve the design problems in two large-scale WDNs. Zheng *et al.* [9] calculated and improved the Pareto-optimal front with a decomposed WDN. Berardi *et al.* [10] detected the vulnerable position in a WDN considering both pipe and node failure. The multi-objective genetic algorithm was used to optimize the network structure and provide guidance on reliability enhancement. Gheisi *et al.* [11] measured the damage tolerance of WDNs considering the maximum number for component-failure scenarios. Di Pierro *et al.* [12] proved that the WDNs in Southern Italy and UK optimized using hybrid algorithms ParEGO and LEMMO, respectively, which improved the efficiency in large-scale WDN design.

However, WDNs are sensitive and vulnerable to disasters [13]. The failure spread and propagation are variances because of the network structure and resources delivered. In studies on anti-disaster ability, cascading failure has been identified as a hotspot in network behavior security. A cascading failure is a dynamic failure process [14]. A small disturbance in the network may result in a large-scale failure, where the small disturbance is always triggered by natural or man-made disasters. The capacity evaluates the largest impact that a node or an edge could bear. However, this capacity is limited according to the budget. That is, if the small disturbance arouses a larger demand that is higher than the node or edge capacity, a new failure situation is created, and the processes continue until the whole network returns to a new stable state.

Although cascading failure was first identified in network behavior, researchers proved that cascading failure also exists in critical infrastructure systems, especially in power grids [15]–[18] and transportation networks [19]–[23]. However, there are few studies on cascading failure in WDNs as most of the pipes are underground. Sitzenfrei *et al.* [24] built a cascading risk map using a geographic information system. The map combined disaster and cascading vulnerability and proved that ignoring cascading failure leads to the underestimation of risks. Yazdani *et al.* [25] showed that WDNs were spatial organized networks. They measured network structure, efficiency, and connectivity of a complex network considering the WDN structure and vulnerability. Yazdani *et al.* [26] quantified the redundancy and failure tolerance. The topology metrics could only describe the network structure, but not the network characteristics related to resources and flow. Hawick [27] explored the concern that WDNs have developed into highly complex networks. Yazdani *et al.* [28] introduced network analysis technology to assess the relationship among network connectivity, system reliability, and failure sensitivity. Shuang *et al.* [29] identified the critical pipe that dramatically reduces system reliability, considering system reliability and cascading propagation time.

Determining the response and reducing the losses during a disaster is an urgent problem that both the governments and society need to address. An efficient strategy is to simulate and optimize the propagation process of cascading failures in WDNs. This strategy will helps prevent and control failure spread. The minimization of cost and total pressure deficit are considered as two objectives. In this study, two optimization scenarios are built: (8) the classical optimization scenario and the cascading optimization scenario. Two benchmark WDNs are considered to illustrate the differences between these scenarios. The Pareto-optimal front was obtained using the particle swarm optimization algorithm. The proposed optimization design solutions will help planners and decision makers to determine the most cost-effective strategy to resist cascading failures, strengthen WDNs, and ensure stable water supply.

II. PROBLEM FORMULATION

The objective functions are formulated as the minimization of the total capital costs and the total hydraulic pressure deficit with a selection of pipe diameter options as the decision variables. The pipe layout, nodal demand, minimum head requirements, and the commercially available diameters are assumed known. Then, the optimization problem of a WDN can be defined as follows:

Find the least cost and least pressure deficit combination of pipe diameters while satisfying the following conditions.

- Conservation of mass: Inflows and outflows must be balanced at each node.
- Conservation of energy: Head loss in each closed loop that begin and end at the same point must be zero.
- The head loss across each pipe is calculated by a function of pipe diameter, pipe length, and material.
- Minimum pressure constraint: Pressure of each node should not less than the minimum pressure.
- Available pipe diameters: Diameters are selected from the commercially available set.

The mathematical formulation of optimization is as follows.

$$\text{minimize}: \quad \mathrm{C} = \sum_{i=1}^{np} f\left(D_i,\ L_i\right) \tag{1}$$

$$\min imize: \quad \mathrm{P}_d = \sum_{j=1}^{nn} \max\left(P_{\min} - P_j\right) \tag{2}$$

$$\text{subject to} \quad \sum \mathrm{Q}_{in} - \sum \mathrm{Q}_{out} = Q_e \tag{3}$$

$$\sum\nolimits_{k\in loop_l} \Delta H_k = 0 \tag{4}$$

$$\sum_{i\in I_p} H_{L,i} + \sum_{j\in J_p} H_{p,j} = \Delta E \tag{5}$$

$$H_L = KQ^{1.852} = 10.654\left(\frac{Q}{C}\right)^{1.852}\frac{1}{D^{4.87}}L$$

$$\mathrm{P}_j > \mathrm{P}_{j,\min} \tag{6}$$

$$\mathrm{D}_i \in D \tag{7}$$

where Eq. (1) describes the first objective function—the minimization the total costs. C is the total cost the WDN; D_i, the diameter of the ith pipe selected from the commercially available set $\{D\}$; L_i, the length of the ith pipe; and np, the number of pipes. Eq. (2) describes the second objective function—the minimization of the total hydraulic pressure deficit. In this equation, P_d is the total hydraulic pressure deficit; $P_{j,min}$, the minimum required pressure at node j; H_j, the simulated pressure at node j; and nn, the number of nodes. Eq. (3) represents the conservation of mass for each junction node. The inflows and outflows must be balanced. Q_{in} and Q_{out} are the pipe inflow and outflows of the node, respectively. Q_e is the external demand or supply. Eq. (4) represents the conservation of energy for each closed loop; here, ΔH_k is the head loss in pipe k. Eq. (5) expresses the head loss along each pipe. In this equation, $H_{L,i}$ is the head loss across pipe i; $H_{p,j}$, the head added by pump j; and ΔE, the difference in energy between the points of pipe. The Hazen–Williams equation is introduced to compute friction H_L. Eq. (6) requires that the nodal pressure P_j is greater than or equal to the minimum pressure $P_{j,min}$. Eq. (7) requires that pipe diameter D_j belongs to the commercially available pipe set D.

III. CLASSICAL OPTIMAL AND CASCADING FAILURE SCENARIOS

Two scenarios are considered in this study—the classical optimal scenario and cascading failure scenario. In the classical optimal scenario, a WDN is optimized to meet multiple objectives with selected pipe diameters. Cascading failures involve a conductive failure process [14]. Shuang *et al.* [30] proved that cascading failures exists in WDNs and can reduce WDN performance drastically.

Urban expansion may be one cause of cascading failures. For example, the water demand has increased because of the sharp rise in population and industries. The nodal demand pattern is much more intensive than the initial design, and it requires the WDN to supply large-scale or high-pressure water. In this case, the nodes in the WDN perform well in the original design but do not meet the new requirements.

A comparison between these two scenarios is provided in Section IV. Case Study for a small and medium-size benchmark WDN.

A. GRAPH REPRESENTATION

A WDN is a network containing connected pipes and other appurtenances to supply, store, and convey water for given demand and pressure requirements. One way to model the structure of a WDN is to use a mathematical graph with node-edge representation [26]. Nodes represent components at specific locations, such as reservoirs, tanks, and consumer junctions. Edges represent pipes and express the connectivity between nodes.

A mathematical graph is represented as $G = G(V, E)$, where V is the set of nodes, and E is the set of edges. A WDN can be considered as a directed graph owing to its flow and pressure requirements. Usually, the incidence matrix (A) is introduced to show the topological structure. A_{ij} shows the connectivity relationship between node i and edge j, and it is used in the hydraulic analysis process to update flow direction. A_{ij} is defined as follows.

$$\mathrm{A}_{ij} = \begin{cases} 1, & \text{Node } i \text{ is the initial node of edge } j \\ -1, & \text{Node } i \text{ is the terminal node of edge } j \\ 0 & \text{Node } i \text{ is the unconnected node of edge } j \end{cases} \tag{8}$$

B. PARAMETER SETTING

A cascading failure can be observed by considering the capacity and load. Load is defined as the network flow that is transferred between the network components. A WDN is a physical network with resource supply and constrains. It has to balance the water supply and water demand according to its network structure. The nodal pressure is a metric that is related to the hydraulic characteristic. Nodes will be fully supplied if the nodal pressure is greater than the service pressure [31]. The service pressure is selected as the initial load.

Capacity is defined as the maximum load that can be borne by a component in the network. A failure in the WDN may trigger flow redistribution [30]. If the load is larger than the capacity, the node fails to supply water.

The maximum capacity is defined as

$$\mathrm{P}_{k,\max} = (1+\alpha)\mathrm{P}_{k,ser} \tag{9}$$

where $P_{k,ser}$ is the service pressure of node k under normal conditions. Here, $\alpha > 0$ is the tolerance parameter and indicates the extra head that a node in the WDN can bear. A high nodal pressure may increase the risk of leakage, while an extremely high nodal pressure may lead to pipe bursts. The nodal pressure should be controlled within a reasonable range to ensure effective WDN operation.

C. EDGE-BASED FAILURE

Failures are usually classified as random failures and targeted failures. Random failures generally refer to external or internal threats, such as natural disasters and human-made damage, and their impacts on the WDNs, for instance, component failures. Random failures have been widely studied [32]–[34]. Although infrastructure systems are robust to random failures, they are extremely vulnerable to targeted

failures [35], [36]. Targeted failures usually refer to failure of certain components under cyber, chemical, and biological attacks [37]. The failure of some critical nodes or pipes will make the entire WDN vulnerable.

Therefore, in this study, the focus is on target failures. The target failures are further classified into node-based and edge-based failures, which refer to failures that start from a node and an edge, respectively. Since pipe failure is more common in WDNs, edge-based failures are simulated in this study.

D. PRESSURE-DRIVEN ANALYSIS

The nodal pressure under normal and failure conditions are simulated by hydraulic engine EPANET 2. EPANET 2 [38] is developed by the US Environmental Protection Agency. It has been widely adopted in hydraulic calculation and water quality simulation. EPANET 2 Programmer's Toolkit can be easily combined with other commercial software. In this study, MATLAB is used to call EPANET 2 Toolkit functions.

EPANET 2 follows the demand-driven analysis. In this analysis, the assumption is that the node demand can always be satisfied. However, water supply and demand change constantly. Under failure conditions, the supply cannot meet the requirement of demand. In this case, the actual demand may less than the required demand under the pressure-deficient condition.

The pressure-driven analysis assumes that the demands depend on pressure, thereby providing a more realistic calculation. A WDN performs normally if all the imposed demands meet with pressures above the service pressure. If the pressure is lower than the service pressure but higher than the minimum pressure, the node cannot supply the full demand, which means that node supplies at a reduced level. Wagner's model [31] has been proven to provide good performance in describing the actual water demand in a pressure-driven analysis [39], [40]. Hence, this model is used for the pressure-driven analysis. Wagner's model is expressed as follows:

$$Q_{k,act} = \begin{cases} 0 & P_k \le P_{k,\min} \\ Q_{k,req}\sqrt{\dfrac{P_k - P_{k,\min}}{P_{k,ser} - P_{k,\min}}} & P_{k,\min} < P_k < P_{k,ser} \\ Q_{k,req} & P_{k,ser} \le P_k \end{cases} \tag{10}$$

where $P_{k,min}$ is the minimum pressure of node k; $P_{k,max}$, the maximum pressure; $P_{k,ser}$, the service pressure; P_k, the calculated node pressure; $Q_{k,act}$, the actual demand; and $Q_{k,req}$, the required water demand.

E. ASSUMPTIONS AND SIMULATION PROCESS

The assumptions of the cascading failure model for a WDN are as follows:

Node: Nodes have effective supply, failure, and pressure-deficient states. In the effective supply state, the nodal pressure is neither higher than the maximum pressure, nor lower than the minimum pressure. In the failure state, the nodal pressure is either higher than the maximum pressure, or lower than the minimum pressure. In the pressure-deficient state, the node pressure is lower than the service pressure but higher than the minimum pressure.

Pipe: Pipes have effective supply and failure states. In the former, water can be transferred from the initial node to the terminal node, while in the latter, the pipe cannot transfer water.

Multi-failure scenario: Failure of one pipe may lead to the failure of several pipes or nodes. For example, if the pipe connecting the source node, such as a tank or reservoir, and the demand node fails, the following nodes will lose their function. In the model, a pipe may trigger the failure of several nodes. These failed nodes will further lead to the failure of other pipes. The failure condition depends on the topological and hydraulic analysis.

Stable condition: A WDN is in the stable condition until no new failed pipe or node is generated.

EPANET Toolkit is called using MATLAB, and the basic information in a WDN, such as the topological structure, node elevation, base demand, pipe diameter, pipe length, and pipe material, are read. The service pressure under the normal condition is obtained using EPANET. The demand multiplier is introduced to analyze the supply and demand relationship. Further, the tolerance parameter helped calculate the maximum pressure.

The pressure deficit is the average value of the total pressure deficit of each pipe with regard to cascading failures. Initial failure starts from a certain pipe. Three analyses are performed for the cascading failure process: (1) The failed component that is disconnected with others is identified by isolation detection. For example, a pipe is an isolated pipe if both its nodes, i.e., the initial and terminal nodes, fail. (2) The components states are simulated, and nodal pressure and flow under failure condition are calculated in a hydraulic analysis. The subsequent failure node is recognized according to the node failure state. The actual demand of this node is set as zero. (3) The network structure is updated via a topological analysis. The incidence matrix is updated with the flow direction. The pipes that are connected to the subsequent failure nodes are set as the new failure components. The processes are simulated until the WDN attained a new stable condition, i.e., no new failure components are found. The total hydraulic pressure deficit is calculated according to the actual and required demands for this new stable state of the WDN.

IV. PARTICLE SWARM OPTIMIZATION

PSO is inspired by the behavior of a flock of birds. PSO performs discrete multi-dimensional searches. Each particle is affected by both the global optimal individual and the local optimal individual. The historical optimal record found by the particle is combined with global searching to attain convergence. The PSO can attain convergence with high speed in single-objective optimization [41]. Coello *et al.* [42] developed an extended PSO to deal with multi-objective optimization problems. They used a secondary repository of particles to guide the flight of other particles. A mutation

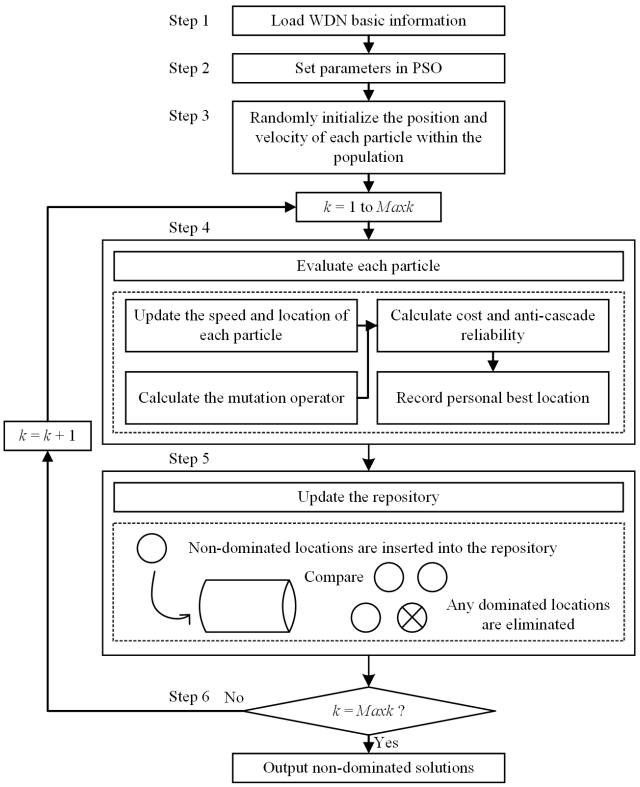

FIGURE 1. Flowchart of multi-objective particle swarm optimization.

operator is added to enrich the exploratory ability. The extend PSO is validated to realize high performance in exploring the full Pareto front with lower computational times than other standard multi-objective optimization algorithms. Therefore, the multi-objective PSO algorithm proposed by Coello *et al.* is used in this study to examine the minimum cost and maximum pressure deficit. Figure 1 shows the optimization flowchart.

Step 1 (Load Basic Information of the WDN): Input the pipe lengths, roughness coefficients, node elevations, base demands, demand multiplier, and network structure.

Step 2 (Set Parameters in PSO): Diameters of the pipes in the WDN are the decision variables. The decision interval is the commercial standard pipe diameter. The diameter of each pipe is set as a solution with particles to search.

Step 3 (Randomly Initialize the Position and Velocity of EACH Particle Within the Population): Copy the particle set into the population matrix. Initialize the particles to generate the initialization matrix. Calculate the cost and pressure deficit according to the particle initialization matrix

Step 4 (Evaluate Each Particle):

(1) Update the speed and location of each particle.

Calculate the speed of each particle:

$$v_i = wv_i + c_1 r_1 (pbest_i - x_i) + c_2 r_2 (rep_h - x_i) \quad (11)$$

Calculate the location of each particle:

$$x_i = x_i + v_i \quad (12)$$

where w is the inertial weight; c_1 and c_2 are the personal learning coefficient and group learning coefficient, respectively; r_1 and r_2 are random numbers between 0 and 1; *pbests* is the personal best position of particle i; *rep* is the global best position; and rep_h is a leader value selected from the repository.

Searching is started from a dominant particle from the nondominant solutions. The velocity and position of each particle are computed. The updated particle position is controlled within the search space. If a decision variable goes beyond the boundary, it is assigned the lower or upper boundary, and its velocity is multiplied by (-1) to search the opposite direction.

(2) Mutation operator

Calculate the mutation operator:

$$po = \left(1 - \frac{k-1}{Maxk-1}\right)^{\frac{1}{\mu}} \quad (13)$$

where po is the mutation operator; k, the current number of iterations; $Maxk$, the total number of iterations; and μ, the mutation rate. Although PSO has high convergence speed, it may converge to a local optimum. Here, the mutation operator motivates more particles to explore the Pareto front.

A random number is generated for each particle. If this random number is less than the mutation operator, the location of a particle is mutated. The cost and pressure deficit are calculated with the original and mutated particle, respectively. The *pbest* is the dominant one among the original and mutated particle.

Otherwise, if the random number is greater than or equal to the mutation operator, no mutation is performed.

Step 5 (Update the Repository): The non-dominated locations are inserted into the repository. A new repository is generated with all non-dominated locations after comparing the updated and existing locations. Any dominated locations in the repository are eliminated. An adaptive grid [43] is generated to produce well-distributed Pareto fronts. The grid has to be recalculated if a solution is located outside the current bounds. Therefore, the grid ensures that all solutions are well located.

Step 6 (End the Search): If the required accuracy or the number of iterations is reached, the search is stopped. The Pareto fronts are drawn with the adaptive grid. The results with non-dominated solutions are converted into a matrix.

Otherwise, if the required accuracy or number of iterations is not attained, step 4 is repeated, and the number of iterations increases.

V. CASE STUDY

The classical optimization scenario and the cascading failure optimization scenario are investigated for two well-known WDNs, namely, the two-loop network (TLN) and the Hanoi network (HAN).

A. TWO-LOOP WDN

The TLN was originally presented by Alperovits and Shamir [44]. The network layout is shown in Figure 2.

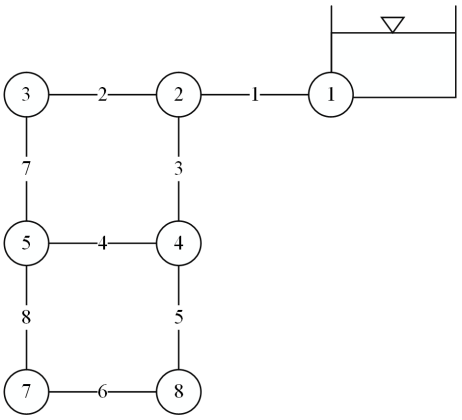

FIGURE 2. Layout of the two-loop network (TLN).

TABLE 1. Data for two-loop network (TLN).

Node	Demand (m^3/h)	Elevation (m)	Node	Demand (m^3/h)	Elevation (m)
1(source)	-1,120	210	5	270	150
2	100	150	6	330	165
3	100	160	7	200	160
4	120	155			

TABLE 2. Cost data for TLN.

Diameter (in.)	Diameter (mm)	Cost (units)	Diameter (in.)	Diameter (mm)	Cost (units)
1	25.4	2	12	304.8	50
2	50.8	5	14	355.6	60
3	76.2	8	16	406.4	90
4	101.6	11	18	457.2	130
6	152.4	16	20	508	170
8	203.2	23	22	558.8	300
10	254	32	24	609.6	550

TLN data are provided in Table 1. The TLN consists of eight pipes organized in two loops, six demand nodes, and one reservoir with a 210.0 m fixed head. The length of each pipe is 1000 m. The minimum pressure is 30 m above the ground level for each node. The Hazen–Williams coefficient C is 130 for each pipe with $w = 10.5088$. Commercially, 14 pipe diameters, ranging from 25.4 mm (1.0 in) to 609.6 mm (24 in) are available. The search space is equal to 14^8 different network designs. The pipe costs are listed in Table 2.

B. HANOI NETWORK

The HAN was first presented by Fujiwara and Khang [45]. The network layout is shown in Figure 3, and HAN data are listed Table 3. The HAN consists of 32 nodes, 34 pipes, and three loops. It has one reservoir with a 100.0 m fixed head. The minimum pressure is 30 m above ground level for each node. The Hazen–Williams coefficient C is 130 for each pipe. In all, six pipe diameters, ranging between 304.8 mm (12 in) and 1016 mm (40 in) are commercially available. The search space is equal to 6^{34} different possible network designs. The pipe costs are listed in Table 4.

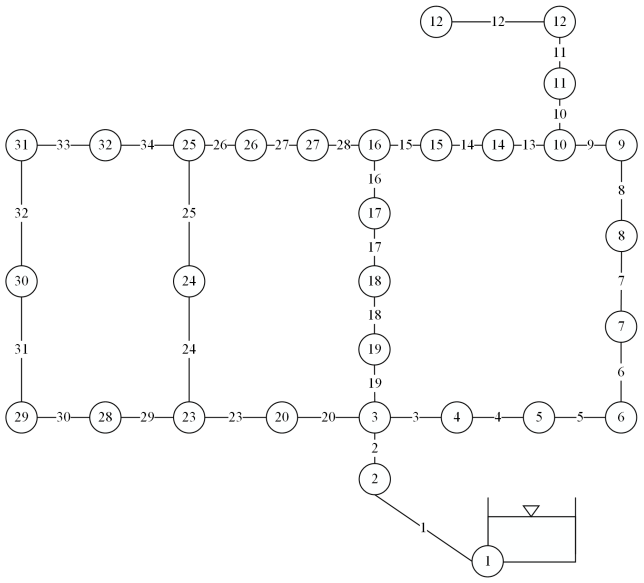

FIGURE 3. Hanoi network (HAN) layout.

TABLE 3. Data for Hanoi network (HAN).

Node	Demand (m^3/h)	Node	Demand (m^3/h)	Pipe	Length (m)	Pipe	Length (m)
1(source)	-19,940	17	865	1	100	18	800
2	890	18	1,345	2	1,350	19	400
3	850	19	60	3	900	20	2,200
4	130	20	1,275	4	1,150	21	1,500
5	725	21	930	5	1,450	22	500
6	1,005	22	485	6	450	23	2,650
7	1,350	23	1,045	7	850	24	1,230
8	550	24	820	8	850	25	1,300
9	525	25	170	9	800	26	850
10	525	26	900	10	950	27	300
11	500	27	370	11	1,200	28	750
12	560	28	290	12	3,500	29	1,500
13	940	29	360	13	800	30	2,000
14	615	30	360	14	500	31	1,600
15	280	31	105	15	550	32	150
16	310	32	805	16	2,730	33	860
				17	1,750	34	950

TABLE 4. Cost data for HAN.

Diameter (in.)	Diameter (mm)	Cost (units)	Diameter (in.)	Diameter (mm)	Cost (units)
12	304.8	45.726	24	609.6	129.333
16	406.4	70.400	30	762.0	180.748
20	508.0	98.378	40	1016.0	278.280

C. CLASSICAL OPTIMAL SCENARIO OPTIMIZATION RESULTS

The PSO solutions of TLN are shown in Figure 4. The least-cost solution (419,000 units) is the identical to the solutions

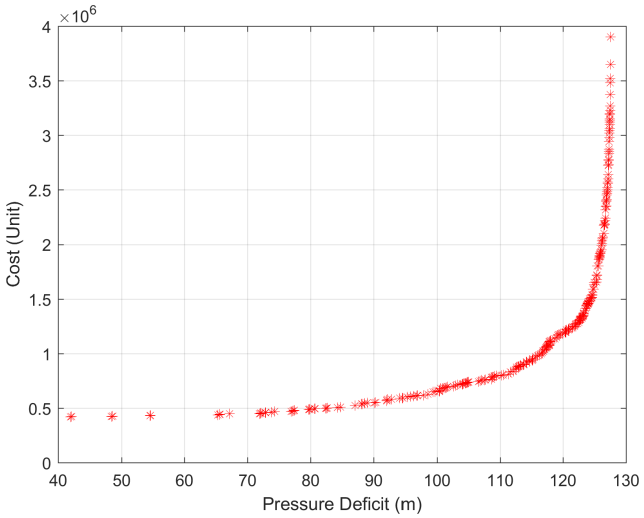

FIGURE 4. Pareto fronts of the TLN problem.

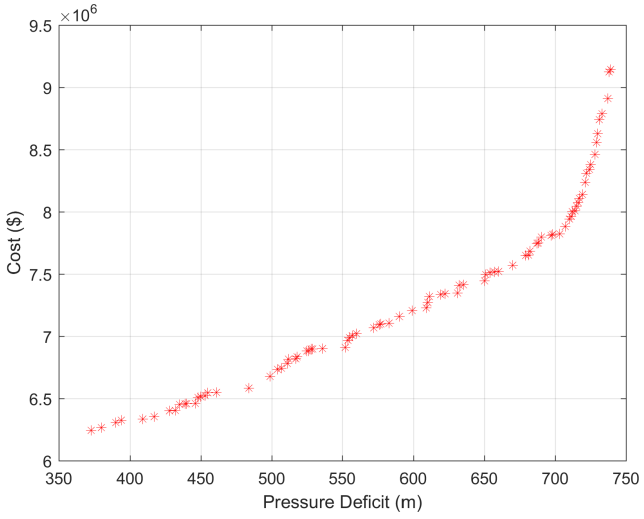

FIGURE 5. Pareto fronts of the HAN problem.

obtained by Savic and Walters [3], Cunha and Sousa [46], Eusuff and Lansey [1], Liong and Atiquzzaman [47].

The PSO solutions of HAN are shown in Figure 5. The least-cost solution is 6.24 million along with a head deficit of 373 (m). The least-cost solution is lower than that obtained by Fujiwara and Khang (6.32 million) [45].

The results of TLN and HAN problems show that the extended PSO can not only find the optimal solution with the least cost, but also obtain the Pareto fronts, which supply more solutions to meet different design requirements. The Pareto fronts in the classical optimal scenario are used as a base line to confirm the effectiveness of simulation under cascading failure.

D. CASCADING FAILURE SCENARIO OPTIMIZATION RESULTS

Figures 6 and 7 show the Pareto fronts for comparing the performance of TLN and HAN in the classical optimal scenario (COS) and cascading failure scenario (CFS).

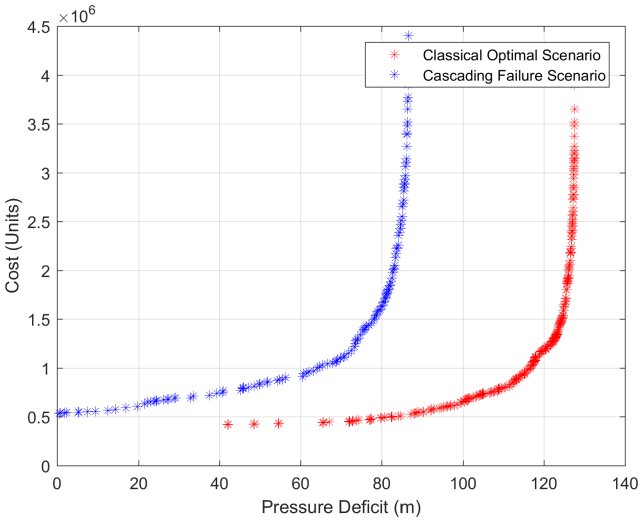

FIGURE 6. Pareto fronts under the cascading failure scenario (CFS) and classical optimal scenario (COS) of the TLN problem.

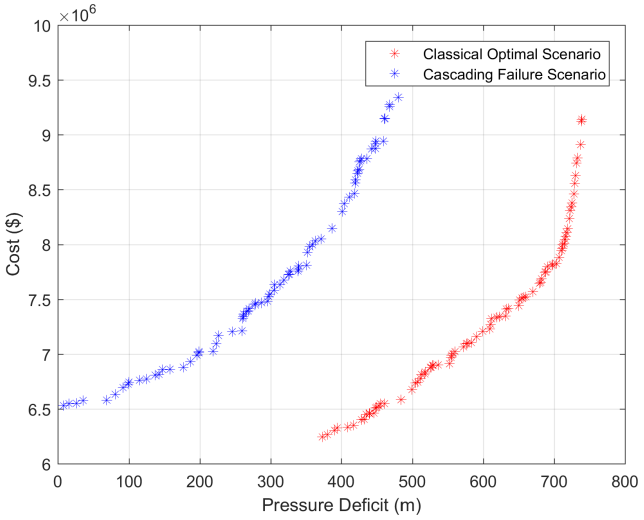

FIGURE 7. Pareto fronts under the CFS and COS of the HAN problem.

To compare the differences between the CFS and COS, the tolerance parameter is set as $\alpha = 30$. This parameter limits the maximum nodal pressure according to Eq. (9). If the nodal pressure is much higher than the service pressure, pipe bursts and leakage are more likely. Hence in this case, the failures caused by high pressure are not considered.

Particles randomly generate the pipe diameter. Only the pipe diameter solutions that meet the minimum nodal pressure requirements can be further tested for CFS simulation. They are used to simulate the cascading failure process, and then calculate the cost and head deficit. Each pipe is selected as an initial target for attack. The head deficit and cost are calculated after the WDN returns to a stable state. All pipes are selected as initial attack targets. The head deficit is the average value of the whole WDN simulated with the failure of each pipe.

The results show that the Pareto front of the COS performs better than that of the CFS. When the nodal pressure deficit is identical for the two scenarios, the cost for the CFS is higher than that for the COS. When the cost is the same, the nodal pressure deficit of the CFS is lower than that of the COS.

In the TLN, the minimum cost under the CFS is 5.35 units, which is higher than that under the COS by 1.16 units. The maximum pressure deficit of the CFS is 86.53 m, which is less than that of the COS by 40.98 m.

In the HAN, the minimum cost under CFS is 6.53 million, which is higher than that under COS by 0.28 million. The maximum pressure deficit of the CFS is 488 m, which is less than that of the COS by 251 m.

The Pareto fronts of the CFS and COS on the small WDN, TLN, and the medium-sized WDN, HAN, show the same trend. Under the CFS, the pressure deficit and cost are reduced, and the identical pressure deficits increases. Cascading failure is a low-probability but high-loss scenario. It may trigger large-scale failure propagation with a small disturbance. A WDN will be vulnerable to cascading failures if only the cost and pressure deficit optimization is considered.

E. COMPARISON OF DIFFERENT TOLERANCE PARAMETERS

The tolerance parameter α expresses the extra pressure that a node can bear. It indicates the aging condition of pipes by expressing their capacity. A larger α indicates a healthier WDN with a higher capacity to resist failure. Nodes can withstand bigger pressure changes. In contrast, a smaller α indicates a higher aging WDN with a decreased capacity. Nodes are sensitive to pressure changes, and they easily lose service functions under excess pressure.

Figure 8 compares the effect of different tolerance parameters to the Pareto font in the TLN under the CFS. The Pareto fronts based on $\alpha = 0.1$, 0.3, 0.5, and 30 are shown in the figure. The TLN is not sensitive to the tolerance parameters. The Pareto fronts are overlapped with different tolerance parameters. It is found that cascading failure will reduce the performance of the WDN. However, the TLN is a small network. The failures will either cause a large-scale loss, or will be absorbed by the network. In this case, the damage caused by cascading failures with different tolerance parameters are not obvious.

Figure 9 shows a comparison of the Pareto fronts with different tolerance parameters for the HAN. The Pareto front with $\alpha = 30$ yields the best performance. Thus, if the WDN has more capacity, less cost is incurred to ensure the same water supply. For example, the required cost is 7 million to ensure a pressure deficit of 200 m. Considering the same pressure deficit, the required cost is 8.31 million ($\alpha = 0.3$) and 8.32 million ($\alpha = 0.3$), which is much larger than the cost corresponding to $\alpha = 0.3$.

If there is only little room in the water supply network, even considering the higher construction cost, the purpose of effectively resisting cascading failure cannot be achieved.

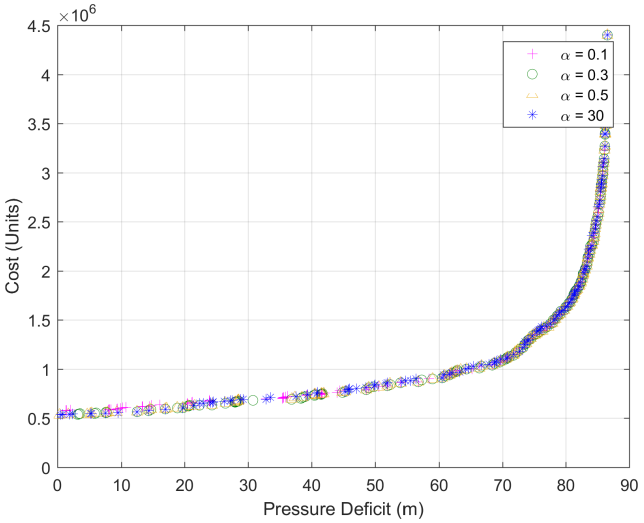

FIGURE 8. Pareto fronts under the CFS and COS for the TLN.

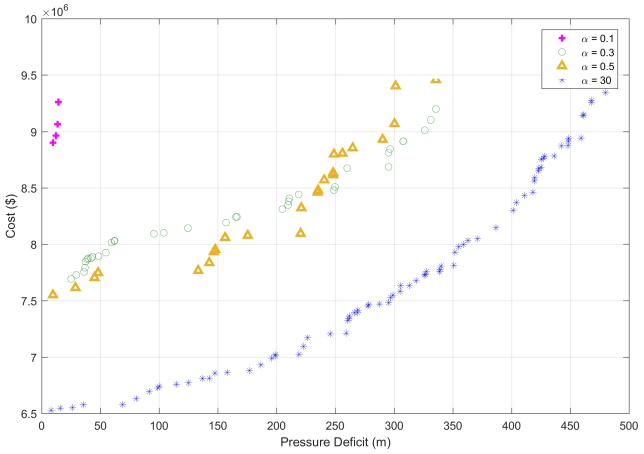

FIGURE 9. Pareto fronts under the CFS and COS for the HAN.

The maximum pressure deficit is only 14.27 m when $\alpha = 0.1$. The number of non-dominated solutions is much lower than those under other conditions. Maintenance is important to ensure the cascading failure resistance of the WDN.

In addition, the Pareto fronts change only slightly for $\alpha = 0.3$ and 0.5. There are overlaps in the case of these two fronts, showing that the aging state of the HAN is not sensitive to cascading failures. There will be a significant change only when α is very small.

Figures 8 and 9 shows that the damage caused by cascading failures to WDN performance. However, different tolerance parameters have different effects corresponding to the size of the WDN. The TLN is a small WDN. Its Pareto fronts for different tolerance parameters are identical. HAN is a medium-sized WDN, and it is sensitive to the tolerance parameters. The smaller the tolerance parameter, the lower is the WDN performance and the higher is the cost for achieving the same performance.

The model provides the Pareto fronts under the COS and CFS. It does not focus on single-objective problems, such as

the minimum cost or maximum pressure deficit. In contrast, the model combines these two objectives and provides a set of nondominant solutions. These solutions present more choices to decision makers. For example, the Pareto fronts can provide solutions with least-cost, maximum functionality, or any solutions that meet the needs of decision makers. The choice of a solution on the Pareto front depends on the urban water demand, municipal budget, and the expectations of decision makers regarding the resilience of the network.

VI. CONCLUSION

A multi-objective optimization model was built for resisting cascading failures in a WDN. The objectives considered both the maximum pressure deficit and the minimum cost. The optimal variables were the pipe diameters. The laws of conservation of mass and energy, nodal pressure, and the standard pipe diameter were set as the constraints.

The Pareto fronts were determined with the extended PSO. Two scenarios—the COS that considers both the maximum pressure deficit and the minimum cost and the CFS—were considered. Only the variables that met the minimum nodal pressure requirement were used to perform the simulation.

Further, two benchmark WDNs were considered—the small TLN and the medium-sized HAN. For the COS, the results showed that both WDNs could find the minimum cost solution. Further, the CFS was tested.

The results for the CFS showed that both WDNs experienced cascading failures. The Pareto fronts under the COS were better than those under the CFS. The pressure deficit and cost were reduced and the same pressure deficit increased. We further tested different tolerance parameters under the CFS. The small TLN was not sensitive to the tolerance parameter. The same Pareto fronts were obtained for different tolerance parameters. However, the medium-sized HAN was sensitive to the tolerance parameter and only a few nondominant solutions were found for $\alpha = 0.1$.

In the future, we wish to explore several aspects. It is interesting that the small- network is not sensitive to the tolerance parameter, but the medium-sized network is. More WDNs should be examined to test the relationship between the network size and the Pareto fronts under the CFS. Further, the edge-based targeted failures were the focus of this study. More failure types, such as leakage and combinations of random and targeted failures should be considered in future research for comprehensive WDN performance evaluation. Besides, multi-objective design problems were considered in this study. The optimal variables were pipe diameters. However, it is impossible to change all pipe diameters in an existing WDN. The critical pipes and their optimal diameters should be determined in future research. This will provide a more realistic solution for maintenance and replacement for WDNs. Back-up operations such as introduction of extra pumps, extra valves, and redundancy network restructures could also be included in the multi-objective problems to obtain more feasible solutions.

REFERENCES

[1] M. M. Eusuff and K. E. Lansey, "Optimization of water distribution network design using the shuffled frog leaping algorithm," *J. Water Resour. Planning Manage.*, vol. 129, no. 3, pp. 210–225, May 2003.
[2] H. Mala-Jetmarova, A. Barton, and A. Bagirov, "A history of water distribution systems and their optimisation," *Water Supply*, vol. 15, no. 2, pp. 224–235, Apr. 2015, doi: 10.2166/ws.2014.115.
[3] D. A. Savic and G. A. Walters, "Genetic algorithms for least-cost design of water distribution networks," *J. Water Resour. Planning Manage.*, vol. 123, no. 2, pp. 67–77, Mar. 1997.
[4] S. H. A. Saleh and T. T. Tanyimboh, "Coupled topology and pipe size optimization of water distribution systems," *Water Resour. Manage.*, vol. 27, no. 14, pp. 4795–4814, Nov. 2013.
[5] E. Zitzler, K. Deb, and L. Thiele, "Comparison of multiobjective evolutionary algorithms: Empirical results," *Evol. Comput.*, vol. 8, no. 2, pp. 173–195, Jun. 2000.
[6] D. Mehdi and A. Asghar, "Pressure management of large-scale water distribution network using optimal location and valve setting," *Water Resour. Manage.*, vol. 33, no. 14, pp. 4701–4713, Nov. 2019.
[7] K. Zhang, H. Yan, H. Zeng, K. Xin, and T. Tao, "A practical multi-objective optimization sectorization method for water distribution network," *Sci. Total Environ.*, vol. 656, pp. 1401–1412, Mar. 2019.
[8] F. Zheng, A. C. Zecchin, J. P. Newman, H. R. Maier, and G. C. Dandy, "An adaptive convergence-trajectory controlled ant colony optimization algorithm with application to water distribution system design problems," *IEEE Trans. Evol. Comput.*, vol. 21, no. 5, pp. 773–791, Oct. 2017.
[9] F. Zheng, A. R. Simpson, and A. C. Zecchin, "An efficient hybrid approach for multiobjective optimization of water distribution systems," *Water Resour. Res.*, vol. 50, no. 5, pp. 3650–3671, May 2014.
[10] L. Berardi, R. Ugarelli, J. Rástum, and O. Giustolisi, "Assessing mechanical vulnerability in water distribution networks under multiple failures," *Water Resour. Res.*, vol. 50, no. 3, pp. 2586–2599, Mar. 2014.
[11] A. R. Gheisi and G. Naser, "On the significance of maximum number of components failures in reliability analysis of water distribution systems," *Urban Water J.*, vol. 10, no. 1, pp. 10–25, Feb. 2013.
[12] F. di Pierro, S.-T. Khu, D. Saviá, and L. Berardi, "Efficient multi-objective optimal design of water distribution networks on a budget of simulations using hybrid algorithms," *Environ. Model. Softw.*, vol. 24, no. 2, pp. 202–213, Feb. 2009.
[13] T. Adachi, "Impact of cascading failures on performance assessment of civil infrastructure systems," Ph.D. dissertation, Georgia Inst. Technol., Atlanta, GA, USA, 2007. [Online]. Available: https://smartech.gatech.edu/handle/1853/14543
[14] A. E. Motter and Y.-C. Lai, "Cascade-based attacks on complex networks," *Phys. Rev. E, Stat. Phys. Plasmas Fluids Relat. Interdiscip. Top.*, vol. 66, no. 6, Dec. 2002, Art. no. 65102.
[15] J.-W. Wang and L.-L. Rong, "Cascade-based attack vulnerability on the US power grid," *Saf. Sci.*, vol. 47, no. 10, pp. 1332–1336, Dec. 2009.
[16] B. Zhou, Y. Lei, C. Li, B. Fang, Q. Wu, L. Li, and Z. Li, "Electrical LeaderRank method for node importance evaluation of power grids considering uncertainties of renewable energy," *Int. J. Electr. Power Energy Syst.*, vol. 106, pp. 45–55, Mar. 2019.
[17] C. Li and Y. Xue, "Effects of cascading failure intervals on synchronous stability," *Int J Elec Power*, vol. 106, pp. 502–510, 2019.
[18] B. Schäfer, D. Witthaut, M. Timme, and V. Latora, "Dynamically induced cascading failures in power grids," *Nature Commun.*, vol. 9, no. 1, p. 1975, Dec. 2018.
[19] H. Liu and J. Wang, "Vulnerability assessment for cascading failure in the highway traffic system," *Sustainability*, vol. 10, no. 7, p. 2333, Jul. 2018.
[20] F. Ma, F. Liu, K. Yuen, P. Lai, Q. Sun, and X. Li, "Cascading failures and vulnerability evolution in bus–metro complex bilayer networks under rainstorm weather conditions," *Int. J. Environ. Res. Public Health*, vol. 16, no. 3, p. 329, Jan. 2019.
[21] A. Candelieri, B. G. Galuzzi, I. Giordani, and F. Archetti, "Vulnerability of public transportation networks against directed attacks and cascading failures," *Public Transp.*, vol. 11, no. 1, pp. 27–49, Jun. 2019.
[22] L. Zhang, J. Lu, B.-B. Fu, and S.-B. Li, "A cascading failures model of weighted bus transit route network under route failure perspective considering link prediction effect," *Phys. A, Stat. Mech. Appl.*, vol. 523, pp. 1315–1330, Jun. 2019.
[23] S. Dong, H. Wang, A. Mostafizi, and X. Song, "A network-of-networks percolation analysis of cascading failures in spatially co-located road-sewer infrastructure networks," *Phys. A, Stat. Mech. Appl.*, vol. 538, Jan. 2020, Art. no. 122971.

[24] R. Sitzenfrei, M. Mair, M. Möderl, and W. Rauch, "Cascade vulnerability for risk analysis of water infrastructure," *Water Sci. Technol.*, vol. 64, no. 9, pp. 1885–1891, Nov. 2011, doi: 10.2166/wst.2011.813.
[25] A. Yazdani and P. Jeffrey, "Complex network analysis of water distribution systems," *Chaos, Interdiscipl. J. Nonlinear Sci.*, vol. 21, no. 1, p. 16111, 2011, doi: 10.1063/1.3540339.
[26] A. Yazdani, R. A. Otoo, and P. Jeffrey, "Resilience enhancing expansion strategies for water distribution systems: A network theory approach," *Environ. Model. Softw.*, vol. 26, no. 12, pp. 1574–1582, Dec. 2011, doi: 10.1016/j.envsoft.2011.07.016.
[27] K. Hawick, "Water distribution network robustness and fragmentation using graph metrics," in *Proc. Int. Conf. Water Resource Manage.*, Sep. 2012, pp. 304–310.
[28] A. Yazdani and P. Jeffrey, "Water distribution system vulnerability analysis using weighted and directed network models," *Water Resour. Res.*, vol. 48, no. 6, Jun. 2012, doi: 10.1029/2012WR011897.
[29] Q. Shuang, Y. Liu, Y. Tang, J. Liu, and K. Shuang, "System reliability evaluation in water distribution networks with the impact of valves experiencing cascading failures," *Water*, vol. 9, no. 6, p. 413, Jun. 2017, doi: 10.3390/w9060413.
[30] Q. Shuang, M. Zhang, and Y. Yuan, "Node vulnerability of water distribution networks under cascading failures," *Rel. Eng. Syst. Saf.*, vol. 124, pp. 132–141, Apr. 2014, doi: 10.1016/j.ress.2013.12.002.
[31] J. M. Wagner, U. Shamir, and D. H. Marks, "Water distribution reliability: Simulation methods," *J. Water Resour. Planning Manage.*, vol. 114, no. 3, pp. 276–294, May 1988.
[32] K. Diao, C. Sweetapple, R. Farmani, G. Fu, S. Ward, and D. Butler, "Global resilience analysis of water distribution systems," *Water Res.*, vol. 106, pp. 383–393, Dec. 2016, doi: 10.1016/j.watres.2016.10.011.
[33] S. Nazif and M. Karamouz, "Algorithm for assessment of water distribution system's readiness: Planning for disasters," *J. Water Resour. Planning Manage.*, vol. 135, no. 4, pp. 244–252, 2009, doi: 10.1061/(ASCE)0733-9496(2009)135:4(244).
[34] B. ZhuangK Lansey and D. Kang, "Resilience/availability analysis of municipal water distribution system incorporating adaptive pump operation," *J. Hydraul. Eng.*, vol. 139, no. 5, pp. 527–537, 2013, doi: 10.1061/(ASCE)HY.1943-7900.0000676.
[35] J. Johansson, H. Hassel, and E. Zio, "Reliability and vulnerability analyses of critical infrastructures: Comparing two approaches in the context of power systems," *Rel. Eng. Syst. Saf.*, vol. 120, pp. 27–38, Dec. 2013.
[36] R. Albert, H. Jeong, and A.-L. Barabási, "Error and attack tolerance of complex networks," *Nature*, vol. 406, no. 6794, p. 378, 2000, doi: 10.1038/35019019.
[37] Y. Y. Haimes, N. C. Matalas, J. H. Lambert, B. A. Jackson, and J. F. R. Fellows, "Reducing vulnerability of water supply systems to attack," *J Infrastruct. Syst.*, vol. 4, no. 4, pp. 164–177, 1998, doi: 10.1061/(ASCE)1076-0342(1998)4:4(164).
[38] L. A. Rossman, "EPANET 2: Users manual," Nat. Risk Manage. Res. Lab., Office Res. Develop., U.S. Environ. Protection Agency, Cincinnati, OH, USA, Tech. Rep. EPA/600/R-00/057, 2000.
[39] O. Giustolisi and T. M. Walski, "Demand Components in Water Distribution Network Analysis," *J Water Res Plan Man*, vol. 138, no. 4, pp. 356–367, 2012, doi: doi:10.1061/(ASCE)WR.1943-5452.0000187.
[40] A. Ostfeld, D. Kogan, and U. Shamir, "Reliability simulation of water distribution systems—Single and multiquality," *Urban Water*, vol. 4, no. 1, pp. 53–61, Mar. 2002.
[41] R. C. EberhartY Shi and J. Kennedy, *Swarm Intelligence*. Amsterdam, The Netherlands: Elsevier, 2001.
[42] C. A. C. Coello, G. T. Pulido, and M. S. Lechuga, "Handling multiple objectives with particle swarm optimization," *IEEE Trans. Evol. Comput.*, vol. 8, no. 3, pp. 256–279, Jun. 2004.
[43] J. D. Knowles and D. W. Corne, "Approximating the nondominated front using the Pareto archived evolution strategy," *Evol. Comput.*, vol. 8, no. 2, pp. 149–172, Jun. 2000, doi: 10.1162/106365600568167.
[44] E. Alperovits and U. Shamir, "Design of optimal water distribution systems," *Water Resour. Res.*, vol. 13, no. 6, pp. 885–900, Dec. 1977.
[45] O. Fujiwara and D. B. Khang, "A two-phase decomposition method for optimal design of looped water distribution networks," *Water Resour. Res.*, vol. 26, no. 4, pp. 539–549, Apr. 1990.
[46] M. D. C. Cunha and J. Sousa, "Water distribution network design optimization: Simulated annealing approach," *J. Water Resour. Planning Manage.*, vol. 125, no. 4, pp. 215–221, Jul. 1999.
[47] S. Liong and M. Atiquzzaman, "Optimal design of water distribution network using shuffled complex evolution," *J. Inst. Eng.*, vol. 44, no. 1, pp. 93–107, 2004.

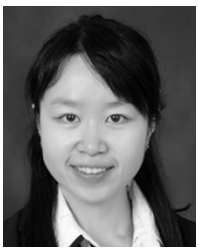

QING SHUANG received the B.Sc., M.Sc., and Ph.D. degrees in civil engineering and management from the Dalian University of Technology.

She is currently an Associate Professor with the Department of Construction Management, School of Economics and Management, Beijing Jiaotong University. She worked as a Visiting Research Scholar at the University of California, Los Angeles, USA, from December 2017 to December 2018. She has authored or coauthored about 20 technical articles and one book. Her major research interests are multi-objective optimization, reliability analysis, and sustainability.

CHAO RAN HUANG received the B.Sc. degree in engineering management from the China University of Mining and Technology, in 2017. He is currently pursuing the master' degree in engineering and project management with the School of Economics and Management, Beijing Jiaotong University.

His current research interests include multi-objective optimization and evolutionary computation.

JUN WANG received the B.Sc. degree in civil engineering management and the M.Sc. degree in civil engineering from the Dalian University of Technology, Dalian, Liaoning, China, in 2010 and 2013, respectively, and the Ph.D. degree in civil engineering from McMaster University, Hamilton, ON, Canada, in 2018.

From January 2017 to May 2017, she worked as a Visiting Research Scholar with the University of Cambridge, U.K. Since August 2018, she has been an Assistant Professor with the Department of Civil and Environmental Engineering, Mississippi State University, USA. Her main research interests are smart and automated construction, sustainable and resilient infrastructure systems, human behaviors and factors, and human-in-the-loop cyber-physical systems.

Dr. Wang is a member of the American Society of Civil Engineers (ASCE), American Society of Safety Professional (ASSP), American Society for Engineering Education (ASEE), and several committees of Transportation Research Board (TRB).